JOURNAL OF SOLID STATE CHEMISTRY 53, 382–386 (1984)

The Structures of Transition Metal–Transition Metal Alloys

JEREMY K. BURDETT AND TIMOTHY J. McLARNAN

Department of Chemistry, The University of Chicago, Chicago, Illinois 60637

Received November 11, 1983; in revised form March 9, 1984

A structure map using the average electron count and *d* orbital energy difference as indices is used to sort transition metal alloys of stoichiometry *AB*. The gross features of the map are mimicked by tight-binding calculations. The inclusion of *s* orbitals on the metal atoms appear to be important in the determination of alloy structure in some parts of the calculated map. The correct coloring of the elemental lattice as a function of electron count is reproduced by calculation (i.e., AuCd vs WC and CsCl vs CuTi). Two new stability fields for the WC and CuTi structures are predicted. The calculations fail to really distinguish bcc, fcc, and hcp derivative structures in the region of 6–8 $d + s$ valence electrons per atom. In this part of the structure map the calculations appear to be sensitive to small geometrical changes.

Introduction

Several years ago the work of Friedel (*1*) and of Pettifor (*2*) led to a description of the electronic and geometrical structures of the transition metals in terms of tight-binding theory. A simple one-electron model is able to faithfully mimic (*2*) the change in crystal structure of the transition metals, and early lanthanide metals as the number of electrons increases. Both qualitative arguments and also detailed calculation (*3*) have shown the overwhelming importance of the *d* electrons in determining the cohesive energies of these metals. The importance of the higher energy *s* and *p* orbitals in influencing the structural, rather than the cohesive part of energy, has been a matter for active debate. The structure maps of Zunger (*4, 5*) and of Machlin and Loh (*6, 7*) have presented diametrically opposing viewpoints. In this paper we will present a new structure map for transition metal–transition metal alloys, show how tight-binding calculations reproduce many of the trends observed in this map, and see how the inclusion of higher energy obitals influences the *d*-only picture.

Structural Sorting

Figure 1 shows a structure map for known alloys of *AB* stoichiometry formed between the transition metals using the indices $\bar{N}$ (the average number of $s + d$ electrons per atom from the Periodic Table) and $\Delta E'$ (the difference in atomic *d* orbital energy between *A* and *B* from the SCF calculations of Herman and Skillman (*8*)). These indices are almost the simplest ones we could have chosen, and the structural sorting, while not perfect, is quite impressive. We have used (*9*) the same parameters to sort *MX* and MX_2 compounds between a

0022-4596/84 $3.00

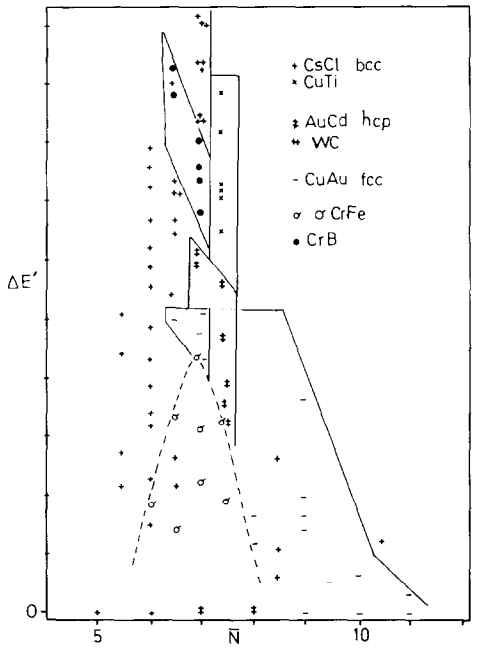

FIG. 1. Landolt–Bornstein database: a structure map for binary transition metal–transition metal alloys of stoichiometry AB, $\bar{N}$ is the average number of valence $s + d$ electrons per atom (obtained from the location of A, B, in the Periodic Table). $\Delta E'$ is the difference in d orbital energy between A, B from the computations of Herman and Skillman (*8*).

transition metal and a main group atom. The map is topologically similar to the one presented by Watson and Bennett (*10*) who used the average number of electron holes and the AB electronegativity difference extracted from experimental studies of the energy bands of the elemental metals. It neither confirms, nor denies the importance of s,p orbitals in controlling crystal structure since the orbital properties of these higher energy orbitals may well be expected to scale with those of the valence d orbitals. It does, however, emphasize the importance of electron count. Of interest are the gross features, (a) the occurrence of the CsCl structure with $\bar{N}$ values which correspond to the region of stability of the elements in the bcc structure, (b) a region with small ΔE where the complex σ phases are found at $\bar{N}$ values corresponding to elemental hcp phases, (c) a sharp line separating the bcc derivative structures CsCl and CuTi at $\bar{N} \sim 7.25$, (d) the observation of the CuAu structure for alloys with $\bar{N}$ values which correspond to the region of stability of the elements in the fcc structure. (Two of the CsCl "errors" in the CuAu region correspond to magnetic phases. Recall that magnetic iron has the bcc but nonmagnetic iron adopts the hcp structure.), (e) a complex region in the middle of the diagram where several stability fields meet, and (f) the positive slope of the bcc/cp boundary at around six electrons and the negative slope of the hcp(σ)/fcc boundary.

Calculated Structure Maps

In order to identify some of the factors behind the choice of alloy structure we have peformed some numerical calculations on these systems using established methods. We were encouraged in this endeavor by the success of Pettifor's calculations (*2*), basically of the Hückel type, which impressively distinguish elemental structures. Figure 2 shows structure maps computed using the tight-binding approach and solving the equation $|H_{ij}(k) - S_{ij}(k)E| = 0$ for the s, p, and d orbital problem at enough k points to reach energetic self-consistency. Slater orbitals were used for s, p, d functions and the hopping matrix elements were estimated using the Wolfsberg–Helmholz approximation. A change in the $\Delta E'$ of Fig. 1 was simulated by increasing all diagonal elements on atom A and decreasing all diagonal elements on atom B by equal amounts. The density of all structural alternatives was required to be the same. (We will return later to this point.) We have no way of assuring that the $\Delta E'$ of Fig. 1 and ΔE of our computed plots are identical and so have used different labels for these two parameters. Calculations were performed on the bcc derivative structures

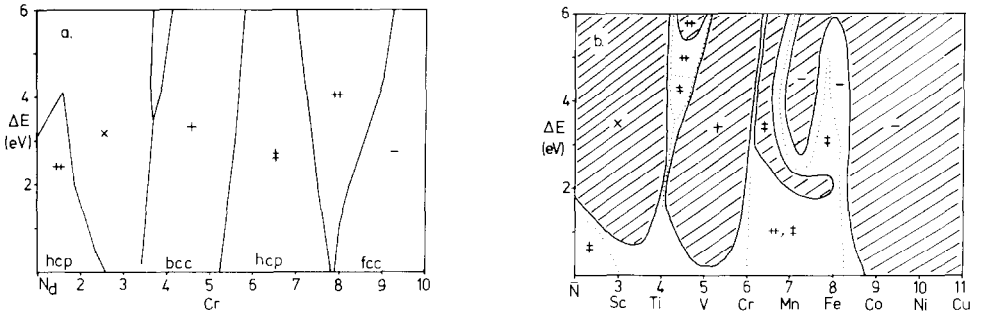

FIG. 2. Calculated structure map for AB alloys using a tight-binding approach (a) nd orbitals only on A, B (b) nd, $(n + 1)s$ and $(n + 1)p$ orbitals on A,B. In (a) the abscissa is the average number of d electrons per atom. In (b) the abscissa is the average number of $(s + d)$ electrons per atom ($\bar{N}$) as in Fig. 1. The symbol key is shown in Fig. 1. In (b) the shaded areas represent regions where the lowest energy structure is at least 0.03 eV more stable than any competitor.

CsCl, CuTi the hcp derivatives WC and AuCd, and the fcc derivative CuAu but were not performed on the CrB or σ phase structures for reasons of computational economy. Notice in both Figs. 1a and b that the correct elemental structural *trend* (namely, hcp–bcc–fcc) is reproduced as the number of electrons increases (compare with Fig. 1). In both plots, however, elemental titanium is erroneously calculated as having the bcc and not the hcp structure. In both sets of calculations too, copper is predicted to have the bcc structure. See the energy difference curves in Ref. (*2*) for example, which are very similar to ours. As in that work we have arbitrarily applied a "hard core" repulsion to remove the discrepancy for cosmetic purposes in Fig. 2. The elemental predictions using this approach do not appear to be overtly sensitive to our choice of orbital parameters or whether d only or $d + s$ or $d + s + p$ orbitals are used on the metal. The metals are assumed (*2*) to have an orbital population $d^n s^1$. In Fig. 3 we show the calculated energy difference curve for the CsCl and CuTi structures as a function of $\bar{N}$. The crossover from the CsCl to CuTi type at about 7.25 electrons which occurs in the experimental map of Fig. 1 is well reproduced. It is masked by a more stable computed hcp structure in the maps of Fig. 2, however. Some of the known CuTi examples have either CuAu or AuCd high temperature forms (*11*). A second CsCl/CuTi changeover is predicted to occur at about 4 electrons and does show up in Fig. 2, but we have no experimental examples to bear it out.

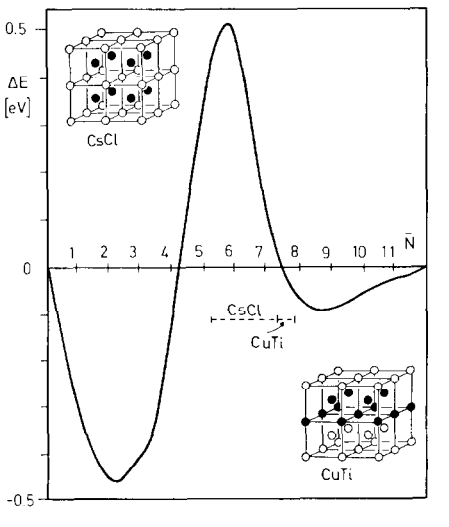

FIG. 3. Energy difference curve between the bcc derivative structures, the CsCl and CuTi arrangements, as a function of $\bar{N}$. The dashed line shows where CsCl and CuTi examples are actually observed.

A curve very similar in shape to that of Fig. 3 is found for the WC and AuCd structures—two colorings of the hcp lattice. As shown in Fig. 2 it is the WC structure which is calculated to be most stable at low band fillings (just as CuTi is calculated to be the preferred bcc derivative at this point). Again, just as in the CuTi/CsCl case, there are no known examples at present to test out our predictions. At around the half-filled band it is the AuCd coloring of hcp which is predicted, and observed to be the more stable variant.

In the region containing the σ phases of Fig. 1, in the calculated maps of Fig. 2 we find no single structure to be overwhelmingly more stable than all the others. Thus it appears that the very complex σ-phase structure occurs almost by default. (Calculations by van der Rest and Giner (*12*) have identified the number of electrons where this phase is stable.) It is also interesting to note that this region, where several structures appear to be very similar in energy is around the magic number suggested by Matthias (*13*) and others (*14*) for the presence of superconductivity. For transition metal–transition metal examples T_c seems to peak[14] at about 6.5 electrons/atom for several different crystal structure types. The presence of a lattice softening for high T_c systems contained in theories of superconductivity may well be related to our energetic observation here.

All the calculations show that the bcc field around six electrons moves to higher $\bar{N}$ as ΔE increases, in agreement with the experimental map. Quantitatively the bcc/fcc crossover at high ΔE is not reproduced very well. Only calculations where the higher energy s or $s + p$ orbitals on the metal are included show the fcc stability field moving to lower $\bar{N}$ as ΔE increases, an important feature of Fig. 1, i.e., inclusion of metal s orbitals while not directly affecting the choice of elemental crystal structure appears to be important in determining alloy structure.

Perhaps the most interesting region of Fig. 1 is that around $\bar{N} = 7.8$ in the middle of the map. Here our calculations are very sensitive to three considerations. The first is the constant volume requirement. Pettifor (*2*) could only get agreement with the observed crystal structure for the elements at the right-hand side of the Periodic Table by adding a hard core repulsion to the bcc energy as we have mentioned above. How large this needs to be for the alloys is unclear since there is a CsCl example with $\bar{N} = 10.5$ in Fig. 1. It may also be the reason behind the lack of observation of the result of Fig. 3 in the calculated maps of Fig. 2. A related problem is concerned with the extra degrees of crystallographic freedom often introduced by the nature of the alloy itself. Thus CuTi has tetragonal symmetry and even within the constant volume restriction the sheet stacking (Fig. 3) need not be equal. We have specifically investigated the importance of this factor by examining the AuCd structure. The calculations of Fig. 2 used the coloring of the hcp lattice itself for this system but the real (orthorhombic) AuCd structure is slightly distorted from this arrangement. The general features of Fig. 2b remain but the region $\sim 6 < \bar{N} < 8$ and $\Delta E > 2$ eV, where AuCd and CuAu structures are very close in energy changes character considerably. This region corresponds to the center of the map of Fig. 1 where several stability fields meet.

Overall then geometrical optimization needs to be undertaken to get really reliable results. This is an area where, unfortunately, calculations of the one-electron type that we have used here, are not at all reliable. As a result we have not undertaken a study of this sort. The third influence on the nature of the map in this region is the inclusion of higher energy orbitals. In calculations performed with d orbitals

alone or with $d + s$ orbitals (at the same or different values of H_{ii}) or with $s + p + d$ orbitals the details of this central region of the map change as shown in Figs. 2a,b.

It is pertinent at this stage to summarize the successes and failures of our series of calculations. First, it is relatively easy to numerically reproduce the *general* structural trends across the transition metal series. Second, we are also able to calculate the lowest energy coloring of an elemental structure[1] namely WC vs AuCd, or CuTi vs CsCl. What is difficult to do using simple theoretical ideas is to accurately discriminate between the close-packed derivative structures. (And also, of course, understand the reasons for the calculated stability of the bcc structures at high band fillings.) This result should not surprise us perhaps since hcp and fcc structures are usually very close together in energy, and it may well take a theory more sophisticated than ours to resolve the problem. It is clear that it is these systems with $\bar{N}$ between ~6 and 8 which will provide the biggest challenge to theorists and provide the most interesting story concerning the factors influencing their structure.

[1] Elsewhere we investigate this coloring problem in a much wider context (see Ref. (*15*)).

Acknowledgments

This research was supported by NSF DMR 8019741. We also thank the donors of the Petroleum Research Fund, administered by the American Chemical Society for its partial support of this research.

References

1. J. FRIEDEL, *in* "Phase Stability in Metals and Alloys" (P. S. Rudman, J. Stringer, and R. I. Jaffee, Eds.), McGraw–Hill, New York (1967).
2. D. G. PETTIFOR, *Calphad* **1,** 305 (1977).
3. C. D. GELATT, H. EHRENREICH, AND R. E. WATSON, *Phys. Rev. B* **15,** 1613 (1977).
4. A. ZUNGER, *Phys. Rev. Lett.* **44,** 582 (1980); *Phys. Rev. B* **22,** 5839 (1980).
5. A. ZUNGER, *Phys. Rev. Lett.* **47,** 1086 (1981).
6. E. S. MACHLIN AND B. LOH, *Phys. Rev. Lett.* **45,** 1642 (1980).
7. E. S. MACHLIN AND B. LOH, *Phys. Rev. Lett.* **47,** 1087 (1981).
8. F. HERMAN AND S. SKILLMAN, "Atomic Structure Calculations," Prentice–Hall, Englewood Cliffs, N.J. (1963).
9. J. K. BURDETT, *J. Solid State Chem.* **45,** 399 (1982).
10. R. E. WATSON AND L. H. BENNETT, *Phys. Rev. B* **18,** 6439 (1978).
11. "Structure Data of Elements and Intermetallic Phases," Landolt-Bornstein, New Series, Vol. 6/III, Springer-Verlag, Heidelberg (1971).
12. J. VAN DER REST AND J. GINER, *Philos. Mag.* **33,** 785 (1976).
13. B. T. MATTHIAS, *Prog. Low Temp. Phys.* **2,** 138 (1957).
14. B. W. ROBERTS, *in* "Intermetallic Compounds" (J. H. Westbrook, Ed.), Wiley, New York (1967).
15. J. K. BURDETT, S. LEE, AND T. J. MCLARNAN, submitted for publication.